http://www.jstage.jst.go.jp/browse/biophysics

BIOPHYSICS

Vol. 9, pp. 167–172 (2013)
doi: 10.2142/biophysics.9.167

Detection of a protein-bound water vibration of halorhodopsin in aqueous solution

Tetsuya Fukuda[1], Kosuke Muroda[1] and Hideki Kandori[1]

[1]*Department of Frontier Materials, Nagoya Institute of Technology, Showa-ku, Nagoya 466-8555, Japan*

Received October 3, 2013; accepted December 4, 2013

Protein-bound water molecules play crucial roles in their structure and function, but their detection is an experimental challenge, particularly in aqueous solution at room temperature. By applying attenuated total reflection (ATR) Fourier-transform infrared (FTIR) spectroscopy to a light-driven Cl^- pump *pharaonis* halorhodopsin (*p*HR), here we detected an O-H stretching vibration of protein-bound water molecules in the active center. The *p*HR(Cl^-) minus *p*HR(Br^-) ATR-FTIR spectra show random fluctuation at 3600–3000 cm^{-1}, frequency window of water vibration, which can be interpreted in terms of dynamical fluctuation of aqueous water at room temperature. On the other hand, we observed a reproducible spectral feature at 3617 (+)/3630 (–) cm^{-1} in the *p*HR(Cl^-) minus *p*HR(Br^-) spectrum, which is absent in the *p*HR(Cl^-) minus *p*HR(Cl^-) and in the *p*HR(Br^-) minus *p*HR(Br^-) spectra. The water O-H stretching vibrations of *p*HR(Cl^-) and *p*HR(Br^-) at 3617 and 3630 cm^{-1}, respectively, are confirmed by light-induced difference FTIR spectra in isotope water ($H_2{}^{18}O$) at 77 K. The observed water molecule presumably binds to the active center of *p*HR, and alter its hydrogen bond during the Cl^- pumping photocycle.

Key words: protein-bound water, membrane protein, ATR-FTIR, hydrogen bond, halide binding

Protein-bound water molecules play crucial roles in their structure and function[1–4]. They may simply occupy an empty space inside protein, but also possibly participate in catalytic reaction of enzyme[1,4] and assist ion-transport inside protein[2]. To investigate the structural role of such internal water molecules, X-ray crystallography is useful, because their atomic positions can be determined. On the other hand, functional role of such molecules is not easily examined. Functional processes accompany dynamical structural alteration of protein, and it is difficult to experimentally detect hydrogen-bonding alteration of internal water molecules during the transient processes. It may be reasonable because water-catalyzed exzymatic reaction and water-associated ion-transport are all short-lived, and unstable intermediate states are hardly detectable.

One exception is seen for photoreceptive proteins, whose transient intermediates can be trapped at low temperatures or kinetically resolved in a time-dependent manner. In fact, we have shown that light-induced difference Fourier-transform infrared (FTIR) spectroscopy is a powerful tool to monitor functional water molecules in photoreceptive proteins such as rhodopsins[2,5,6]. In the measurements, we prepare hydrated films of proteins, by which water content in the sample can be significantly reduced[7,8]. Then, low-temperature or time-resolved difference FTIR spectra provide water O-H (O-D in D_2O) stretching vibrations, which is assigned by use of isotope water (^{18}O)[7,8]. This is an established method, and it is generally accepted that protein dynamics in hydrated films are similar to those in aqueous solution[9,10]. But then, how about protein-bound waters?

Water concentration in aqueous solution is 55 M, and to study a single water molecule bound to 55 μM protein, we have to extract the single water signal out of 10^6 water molecules, which is practically impossible. In the case of hydrated films, typical water content is 1000 molecules per one protein molecule[7,8]. This allows detection of water

Correspondence author: Hideki Kandori, Department of Frontier Materials, Nagoya Institute of Technology, Showa-ku, Nagoya 466-8555, Japan.
e-mail: kandori@nitech.ac.jp

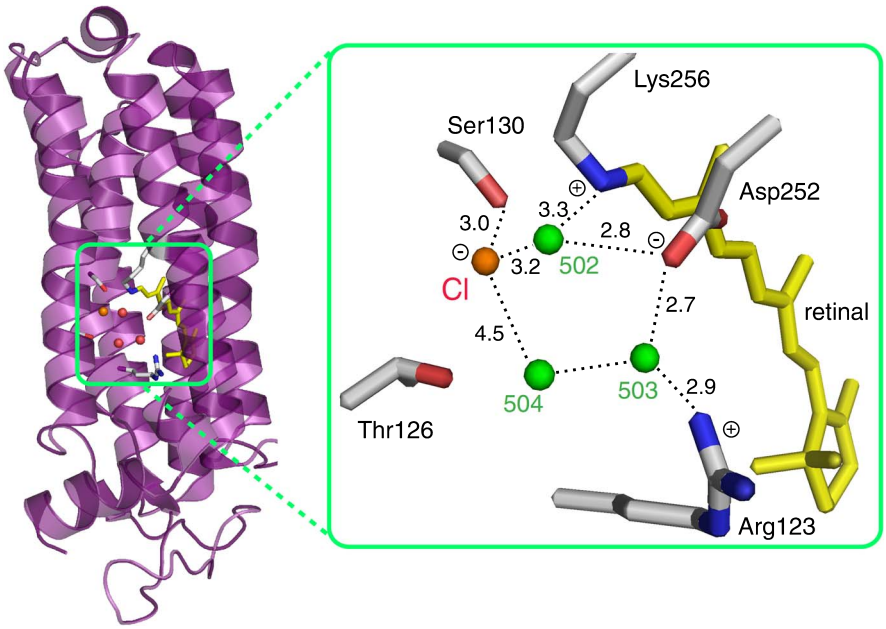

Figure 1 (Left) X-ray crystallographic structure of the *pharaonis* halorhodopsin (*p*HR) (Protein Data Bank entry: 3A7K[17]). For easy view of the active center, the amino-acid residues from Ser37 to Leu 51 in helix A are removed from the structure. The upper and lower regions correspond to the cytoplasmic and extracellular sides, respectively. (Right) Structure of the Schiff base region in *p*HR[17]. Membrane normal is approximately in the vertical direction of this figure, and upper and lower regions correspond to the cytoplasmic and extracellular sides, respectively. Chloride ion, shown by orange sphere, is translocated upward in the figure. Green spheres represent water molecules in the Schiff base region. Dotted lines represent putative hydrogen bonds, whose distances are shown in Å.

stretching vibrations, but protein samples are not filled by aqueous solution. Detection of protein-bound waters in water, not in hydrated films, is a great spectroscopic challenge. Such difficulty may be overcome by applying attenuated total reflection (ATR) FTIR spectroscopy to membrane proteins[11–13]. In the measurements, membrane proteins in lipids are attached on the ATR cell, and buffer solution fills the cell. Then, IR evanescent wave monitors vibrations of the sample in aqueous solution. An important feature is that membrane proteins are accumulated onto the ATR cell surface, so that molar ratio of water molecules per protein is reduced even when proteins are filled in aqueous solution, and functionally important water signals may be extracted by some stumuli, such as different ion binding.

In this paper, we apply ATR-FTIR spectroscopy to *pharaonis* halorhodopsin (*p*HR)[14–17], a light-driven Cl^- pump, and report the successful detection of a water vibration in water by measuring the difference spectra between the Cl^- and Br^- bound forms. Recent X-ray structure of *p*HR showed the presence of three water molecules in the Cl^- binding site of the retinal Schiff base region (Fig. 1)[17]. Therefore, we expected that water signal may be involved in the ion-exchange difference spectra between Cl^- and Br^-, which is indeed the case.

Experimental Procedures

*p*HR was prepared as described previously[15,18], and ATR-FTIR spectroscopy was applied to *p*HR as described[19–21]. The wild-type *p*HR was expressed in *E. coli*, and the purified protein through Ni-column and DEAE-column chromatography was reconstituted into L-α-phosphatidylcholine (egg, Avanti) liposomes[15,18].

The *p*HR sample was first dried on the ATR diamond cell, and filled by perfusion buffer (10 mM MES buffer (pH 6.0) containing 5 mM NaCl or NaBr), Then, Cl^- or Br^- containing buffer (5 mM NaCl or NaBr, 10 mM MES buffer at pH 6.0) was flowed every 20 min at a rate of 0.5 mL/min alternately, during which ATR-FTIR spectra of *p*HR were recorded at 293 K for 15 min (1725 scans) using a Bio-Rad FTS-7000 spectrometer, equipped with a liquid nitrogen cooled MCT detector[19–23]. Spectral resolution was 2 cm^{-1}. It took 40 min to obtain a single *p*HR(Cl^-) minus *p*HR(Br^-) spectrum. We confirmed that the *p*HR(Cl^-) minus *p*HR(Br^-) spectra and *p*HR(Br^-) minus *p*HR(Cl^-) spectra represent mirror images of each other at 1800–800 cm^{-1}, so that the measurements were repeated by changing buffers repeatedly.

Our previous ATR-FTIR reports showed that the difference spectra with and without salt (50 and 0 mM NaCl, respectively) contain significant spectral changes of water molecules and buffer components in addition to the spectral changes of the protein itself, and thus, spectral subtraction was needed to remove such spectral changes[19,20]. In contrast, the obtained spectra in the present study did not contain the spectral components of water molecules and buffer, presumably because of the identical salt concentration. Figure 2a

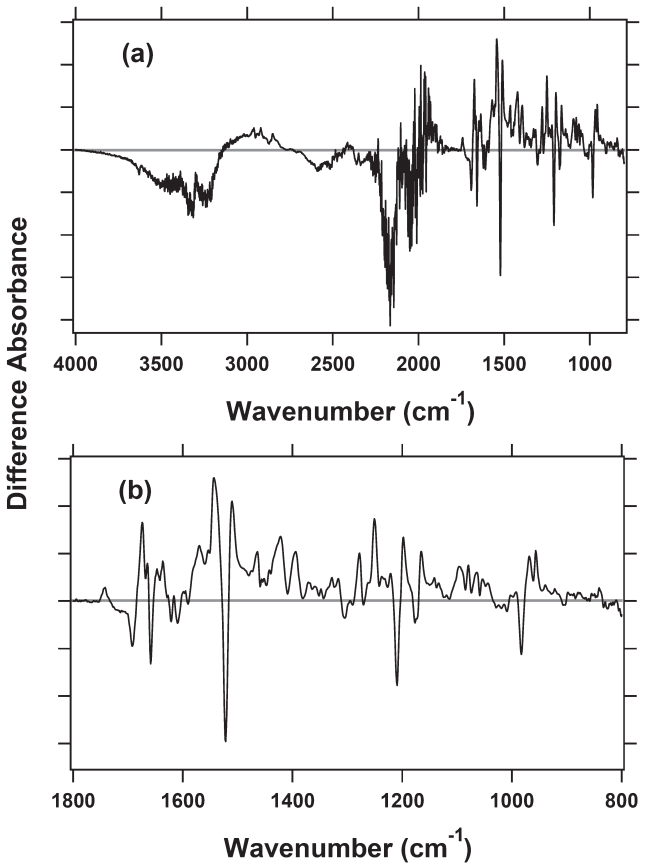

Figure 2 Difference ATR-FTIR spectra between *p*HR(Cl^-) and *p*HR(Br^-) in 4000–800 cm^{-1} (a) and 1800–800 cm^{-1} region (b). In both figures, one division of the y-axis corresponds to 0.0002 absorbance unit.

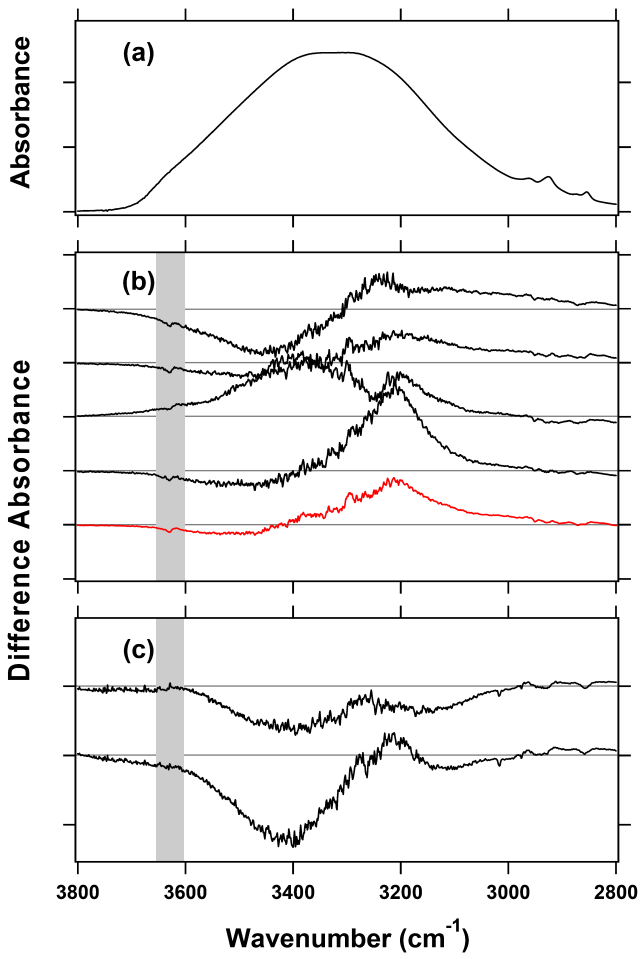

Figure 3 (a) ATR-FTIR spectra of *p*HR in the Cl^- buffer (5 mM NaCl, 10 mM MES at pH 6.0) at 293 K in the 3800–2800 cm^{-1} region. One division of the y-axis corresponds to 0.5 absorbance unit. (b) *p*HR(Cl^-) minus *p*HR(Br^-) difference ATR-FTIR spectra. The top four spectra (black line) represent independent measurements composed of 6 averages of a single difference for each recording of 1725 scans. The bottom spectrum (red line) is the average of the four spectra. One division of the y-axis corresponds to 0.0005 absorbance unit. (c) *p*HR(Cl^-) minus *p*HR(Cl^-) (top) and *p*HR(Br^-) minus *p*HR(Br^-) (bottom) difference ATR-FTIR spectra. The spectra for *p*HR(Cl^-) and *p*HR(Br^-) in (b) are used. One division of the y-axis corresponds to 0.001 absorbance unit.

shows the *p*HR(Cl^-) minus *p*HR(Br^-) difference spectrum in the 4000–800 cm^{-1} region, and the spectral feature in the conventional low frequency region (1800–800 cm^{-1}) (Fig. 2b) was consistent with the previous report[16].

Low-temperature light-induced difference FTIR spectroscopy was applied to hydrated films at 77 K using a Bio-Rad FTS-40 spectrometer, equipped with a liquid nitrogen cooled MCT detector[15,18]. The films were hydrated by 1 µL of H_2O or $H_2{}^{18}O$, and mounted in an Oxford DN-1704 cryostat. The pHR_K (K intermediate) minus *p*HR spectra were obtained by illumination with a 500 nm light (through an interference filter) for 2 min. Three independent measurements with 128 interferograms were averaged.

Results and Discussion

Figure 3a shows absorption spectra of the *p*HR(Cl^-) sample in the 3800–2800 cm^{-1} region, which was measured by ATR-FTIR spectroscopy in aqueous solution. Broad positive spectral feature originates from water O-H stretching vibrations, and smaller peaks at 3000–2800 cm^{-1} correspond to C-H stretching vibrations of PC liposomes and protein. When buffer was changed from Cl^- to Br^-, the absorption spectrum looks identical, and Figure 3b shows the difference between Cl^- and Br^-. The top four spectra in Figure 3b represent independent measurements of 10,350 scans (6 averages of a single difference for each recording of 1725 scans), and the bottom red spectrum of Figure 3b is the average of the four spectra. Each spectrum of the top four in Figure 3b shows difference spectral features at 3600–3000 cm^{-1}, which can be interpreted in terms of fluctuation of aqueous water. In fact, similar spectral features are obtained in the absence of the protein sample. At room temperature, water molecules in aqueous phase quickly change their hydrogen bonds, so that the spectra in this region fluctuate significantly[24]. This means that sufficient averaging will cancel these bands, ideally providing flat spectral feature.

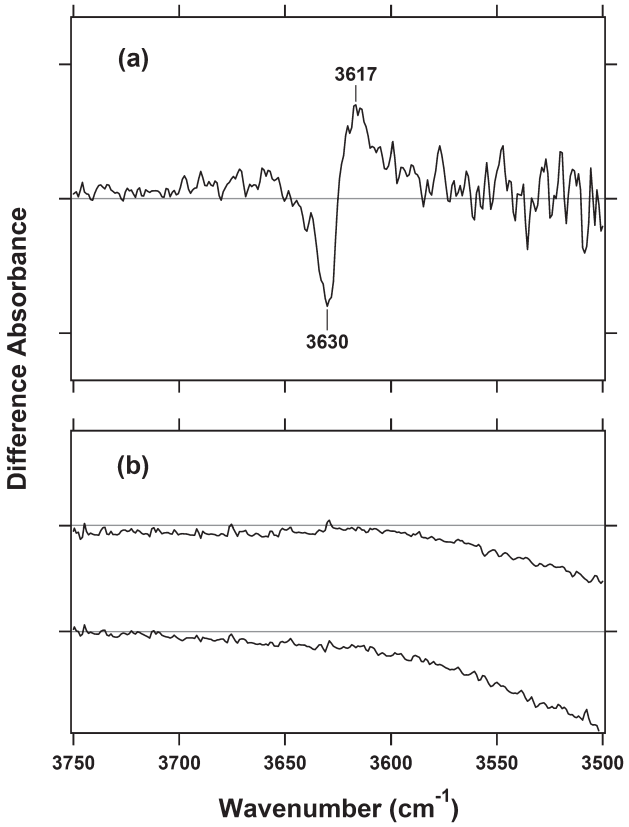

Figure 4 Expanded figure of the red spectrum in Figure 3b (a) and Figure 3c (b) in the 3750–3500 cm^{-1} region, where each spectrum is offset to exhibit the absorbance at 3750 cm^{-1} to be zero. The spectra correspond to the *p*HR(Cl$^-$) minus *p*HR(Br$^-$) (a), *p*HR(Cl$^-$) minus *p*HR(Cl$^-$) (top panel of b), and *p*HR(Br$^-$) minus *p*HR(Br$^-$) (bottom panel of b) differences. One division of the y-axis corresponds to 0.00003 (a) and (b) 0.00008 absorbance unit.

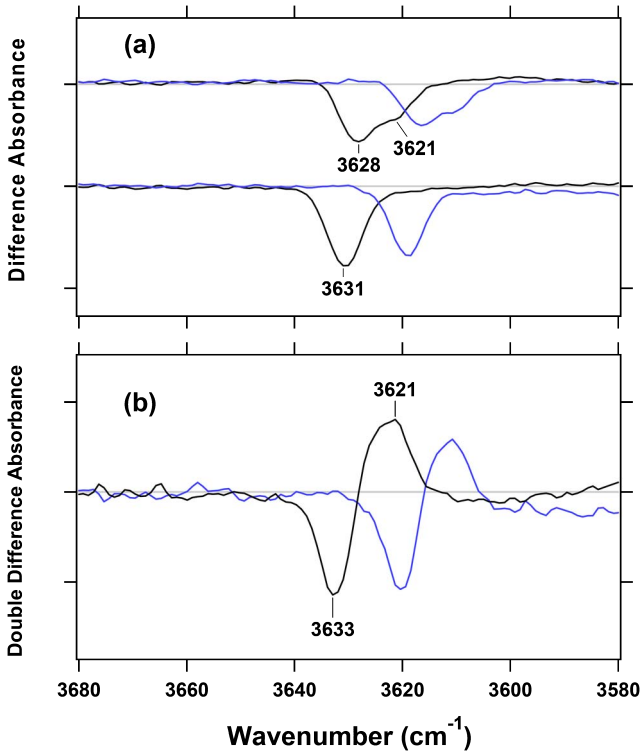

Figure 5 (a) Light-induced *p*HR$_K$ minus *p*HR difference spectra of the Cl$^-$ (top) and Br$^-$ (bottom) bound forms in the 3680–3580 cm^{-1} region. The sample was hydrated with H_2O (black line) and $H_2{}^{18}O$ (blue line), and spectra were measured at 77 K. One division of the y-axis corresponds to 0.0008 absorbance unit. (b) Double difference spectra of a, which correspond to the *p*HR(Cl$^-$) minus *p*HR(Br$^-$) spectra. One division of the y-axis in panel (b) corresponds to 0.0003 absorbance unit.

It should be however noted that data collection for 3 hours (10,350 scans for *p*HR(Cl$^-$) and 10,350 scans for *p*HR(Br$^-$)) was not sufficient to cancel spectral deviation due to water in the scale of 10^{-4} absorbance (Fig. 3b). The spectral deviation between Cl$^-$ and Br$^-$ does not originate from specific water molecules, because similar spectral features were obtained for the differences between Cl$^-$ and Cl$^-$ (top trace in Fig. 3c) and between Br$^-$ and Br$^-$ (bottom trace in Fig. 3c).

While the spectra look randomly fluctuating at 3600–3000 cm^{-1}, we observed a reproducible spectral feature at 3650–3600 cm^{-1} (shaded region in Fig. 3b and c). Figure 4 shows the enlarged figure, which exhibits a clear peak pair at 3630 (–)/3617 (+) cm^{-1} in the *p*HR(Cl$^-$) minus *p*HR(Br$^-$) spectrum (Fig. 4a), but neither in the *p*HR(Cl$^-$) minus *p*HR(Cl$^-$) nor in the *p*HR(Br$^-$) minus *p*HR(Br$^-$) spectra (Fig. 4b). We thus conclude that *p*HR(Cl$^-$) and *p*HR(Br$^-$) possess vibrations at 3617 and 3630 cm^{-1}, respectively. This frequency is characteristic of O-H stretching vibrations, most likely originating from water molecule under very weak hydrogen-bonding conditions (called "dangling bond"). To assign water stretching vibrations, we normally use ^{18}O water ($H_2{}^{18}O$)[2,15]. We need only 1 μL ^{18}O water for the measurements of hydrated films[7,8], but ATR-FTIR measurements require about 1 L buffer for perfusion. Since the measurements are too expensive, here we attempted different approach.

Since *p*HR responds to light, we measured low-temperature light-induced difference FTIR spectra of hydrated films of *p*HR(Cl$^-$) and *p*HR(Br$^-$) at 77 K. If similar vibrational bands are observed, we can confirm similar water environments between aqueous solution and hydrated films, and between room (293 K) and low (77 K) temperatures. Figure 5a shows light-induced difference FTIR spectra of *p*HR(Cl$^-$) (top trace) and *p*HR(Br$^-$) (bottom trace) at 77 K, where positive and negative signals correspond to the K intermediate and unphotolyzed state of *p*HR, respectively. The *p*HR(Cl$^-$) spectrum shows a negative peak at 3628 cm^{-1} with a shoulder at 3621 cm^{-1}, while the *p*HR(Br$^-$) spectrum shows a negative peak at 3631 cm^{-1}. No positive peaks indicate no spectral contribution of the K intermediate at these frequencies. Since these peaks exhibit spectral downshifts by 12 cm^{-1} in $H_2{}^{18}O$ (blue traces in Fig. 5a), these bands originate from water O-H stretching vibrations. The water O-H stretches at 3628 and 3631 cm^{-1} probably correspond to the previously

reported water O-D stretches at 2683 and 2685 cm^{-1}, respectively, in D_2O[15].

Black and blue spectra in Figure 5b are the calculated double difference spectra in H_2O and $H_2{}^{18}O$, respectively, which correspond to the *p*HR(Cl^-) minus *p*HR(Br^-) spectrum. From the spectral coincidence between room temperature (Fig. 4a) and 77 K (black line in Fig. 5b), we concluded that the bands at 3630 (–)/3617 (+) cm^{-1} originate from water O-H stretching vibrations bound to *p*HR. It should be noted that the observed difference absorbance for ATR-FTIR (Fig. 4a) is about one order of magnitude smaller than that for low-temperature light-induced FTIR (Fig. 5b). Smaller signal in ATR-FTIR probably originates from low protein concentration in the measurement, as judged from the amide-II signals (0.18 absorbance for ATR-FTIR and 0.59 absorbance for low-temperature light-induced FTIR). It should be also noted that absorbance in ATR-FTIR decreases at high frequency region because of smaller penetration of evanescent wave, providing smaller amplitude for O-H stretch (~3600 cm^{-1}) compared to amide-II (~1550 cm^{-1}) only in ATR-FTIR. Spectral half widths were 10 and 15 cm^{-1} for the 3630 and 3617 cm^{-1} bands, respectively, for ATR-FTIR (Fig. 4a), while those for low-temperature light-induced FTIR were 6 and 9 cm^{-1} for the 3633 and 3621 cm^{-1} bands (Fig. 5b). These results show that water O-H bands at room-temperature are more broadened than at 77 K, but temperature effect is not significant.

Spectral coincidence of the water bands between 293 and 77 K further provides several suggestions. First, location of the observed water molecule is near the retinal chromophore, because the water changes its hydrogen bond upon retinal photoisomerization at 77 K. Therefore, the water molecule probably originates from one of the three water molecules in Figure 1, and the high frequency implies the water O-H group free from hydrogen bond. The frequency difference between Cl^- and Br^- is probably reflected from that in ionic radius. It should be noted that the proper identification needs comprehensive mutational analysis as we did for a light-driven proton pump bacteriorhodopsin[25]. Second, the water-containing hydrogen-bonding structure in the Schiff base region is structurally persistent from room temperature to 77 K, suggesting the accuracy of X-ray crystal structure that normally obtained at low temperatures[17]. One might predict that the structures of protein-bound water molecules are different between room and low temperatures, but this is not the case for *p*HR (Fig. 4a vs 5b). Interestingly, the water bands are not so broadened at higher temperature, and temperature-independent nature of the water bands suggests the structural rigidity of the active center. Little has been known about the temperature-dependent nature of water O-H stretching vibrations at a single water band level. Therefore, the present study will provide useful information about the molecular property of water. Such water-containing hydrogen-bonding network must play important functional role. In fact, we found strong correlation between the hydrogen-bonding strength of such water molecules and proton-pumping activity of rhodopsins[6,26,27].

Recent time-resolved FTIR spectroscopy of *p*HR under H_2O or $H_2{}^{18}O$ hydration successfully monitored water structural changes during the Cl^- pumping photocycle at room temperature[28]. The observed band at 3626 cm^{-1} for the unphotolyzed state of *p*HR probably corresponds to the positive band at 3617 cm^{-1} in Figure 4a. The water band disappears in the L_1 and L_2 states, while relatively intense positive bands at 3605 and 3608 cm^{-1} emerged upon the formation of the X(N) and O states, respectively[28]. This suggests that the chloride transportation is accompanied by dynamic rearrangement of the hydrogen-bonding network of protein-bound water molecules in *p*HR.

In summary, we report an O-H stretching vibration of protein-bound water molecules in a light-driven chloride pump *p*HR. The *p*HR molecules are embedded in aqueous solution, but ATR-FTIR spectroscopy directly extracts the water signal by monitoring vibrations at the surfaces of the ATR cells. Detection of protein-bound water molecules using ATR-FTIR spectroscopy was also reported for cytochrome c oxidase[29], and the method will be applied to more numerous membrane proteins in future. Since protein-bound water molecules play important role in membrane proteins action, observation of hydrogen-bonding alterations of water helps understanding of molecular mechanism. Useful structural information of protein-bound water molecules will be provided by difference ATR-FTIR spectroscopy.

ACKNOWLEDGMENT

We thank Dr. Y. Furutani, Dr. M. Iwaki, Dr. K. Katayama and Y. Asai for valuable suggestions. Some of the researches described here were supported by grants from Japanese Ministry of Education, Culture, Sports, Science, and Technology.

REFERENCES

1. Kornblatt, J. & Kornblatt, J. The role of water in recognition and catalysis by enzymes. *The Biochemist* **19**, 14–17 (1997).
2. Kandori, H. Role of internal water molecules in bacteriorhodopsin. *Biochim. Biophys. Acta* **1460**, 177–191 (2000).
3. Nicolls, P. Introduction: the biology of the water molecule. *Cell. Mol. Life Sci.* **57**, 987–992 (2000).
4. Pocker, Y. Water in enzyme reactions: biophysical aspects of hydration-dehydration processes. *Cell. Mol. Life Sci.* **57**, 1008–1017 (2000).
5. Kandori, H. Hydration switch model for the proton transfer in the Schiff base region of bacteriorhodopsin. *Biochim. Biophys. Acta* **1658**, 72–79 (2004).
6. Kandori, H. Hydrogen bonds of protein-bound water molecules in rhodopsins. in *Hydrogen bonding and transfer in the excited state* (John-Wiley & Sons Ltd, West Sussex) pp. 377–391 (2010).
7. Furutani, Y. & Kandori, H. Hydrogen-bonding changes of internal water molecules upon the actions of microbial rhodop-

sins studied by FTIR spectroscopy. *Biochim. Biophys. Acta* in press (2014).
8. Yamada, D. & Kandori, H. FTIR spectroscopy of flavin-binding photoreceptors. *Methods Mol. Biol.* in press (2014).
9. Garczarek, F. & Gerwert, K. Functional waters in intraprotein proton transfer monitored by FTIR difference spectroscopy. *Nature* **439**, 109–112 (2006).
10. Lórenz-Fonfría, V. A. & Kandori, H. Spectroscopic and kinetic evidence on how bacteriorhodopsin accomplishes vectorial proton transport under functional conditions. *J. Am. Chem. Soc.* **131**, 5891–5901 (2009).
11. Zscherp, C. & Barth, A. Reaction-induced infrared difference spectroscopy for the study of protein reaction mechanisms. *Biochemistry* **40**, 1875–1883 (2001).
12. Iwaki, M., Puustinen, A., Wikstrom, M. & Rich, P. R. ATR-FTIR spectroscopy of the P_M and F intermediates of bovine and *Paracoccus denitrificans* cytochrome *c* oxidase. *Biochemistry* **42**, 8809–8817 (2003).
13. Nyquist, R. M., Ataka, K. & Heberle, J. The molecular mechanism of membrane proteins probed by evanescent infrared waves. *Chembiochem* **5**, 431–436 (2004).
14. Váró, G. Analogies between halorhodopsin and bacteriorhodopsin. *Biochim. Biophys. Acta* **1460**, 220–229 (2000).
15. Shibata, M., Muneda, N., Sasaki, J., Shimono, K., Kamo, N., Demura, M. & Kandori, H. Hydrogen-bonding alterations of the protonated Schiff base and water molecule in the chloride pump of *Natronobacterium pharaonis*. *Biochemistry* **44**, 12279–12286 (2005).
16. Guijarro, J., Engelhard, M. & Siebert, F. Anion uptake in halorhodopsin from *Natromonas pharaonis* studied by FTIR spectroscopy: consequences for the anion transport mechanism. *Biochemistry* **45**, 11578–11588 (2006).
17. Kouyama, T., Kanada, S., Takeguchi, Y., Narusawa, A., Murakami, M. & Ihara, K. Crystal structure of the light-driven chloride pump halorhodopsin from *Natronomonas pharaonis*. *J. Mol. Biol.* **396**, 564–579 (2010).
18. Nakashima, K., Nakamura, T., Takeuchi, S., Shibata, M., Demura, M., Tahara, T. & Kandori, H. Properties of the anion-binding site of *pharaonis* halorhodopsin studied by ultrafast pump-probe spectroscopy and low-temperature FTIR spectroscopy. *J. Phys. Chem. B* **113**, 8429–8434 (2009).
19. Kitade, Y., Furutani, Y., Kamo, N. & Kandori, H. Proton release group of *pharaonis* phoborhodopsin revealed by ATR-FTIR spectroscopy. *Biochemistry* **48**, 1595–1603 (2009).
20. Sudo, Y., Kitade, Y., Furutani, Y., Kojima, M., Kojima, S., Homma, M. & Kandori, H. Interaction between Na^+ ion and carboxylates of the PomA-PomB stator unit studied by ATR-FTIR spectroscopy. *Biochemistry* **48**, 11699–11705 (2009).
21. Furutani, Y., Murata, T. & Kandori, H. Sodium or lithium ion-binding-induced structural changes in the K-ring of V-ATPase from *Enterococcus hirae* revealed by ATR-FTIR spectroscopy. *J. Am. Chem. Soc.* **133**, 2860–2863 (2011).
22. Furutani, Y., Shimizu, H., Asai, Y., Fukuda, T., Oiki, S. & Kandori, H. ATR-FTIR spectroscopy revealing the different vibrational modes of the selectivity filter interacting with K^+ and Na^+ in the open and collapsed conformations of the KcsA potassium channel. *J. Phys. Chem. Lett.* **3**, 3806–3810 (2012).
23. Doki, S., Kato, H. E., Solcan, N., Iwaki, M., Koyama, M., Hattori, M., Tsukazaki, T., Sugita, Y., Kandori, H., Newstead, S., Ishitani, R. & Nureki, O. Structural basis for dynamic mechanism of proton-coupled symport by the peptide symporter POT. *Proc. Natl. Acad. Sci. USA* **110**, 11343–11348 (2013).
24. Eisenberg, D. & Kauzmann, W. *The structure and properties of water* (Oxford University Press) (1969).
25. Shibata, M. & Kandori, H. FTIR studies of internal water molecules in the Schiff base region of bacteriorhodopsin. *Biochemistry* **44**, 7406–7413 (2005).
26. Shibata, M., Ihara, K. & Kandori, H. Hydrogen-bonding interaction of the protonated Schiff base with halides in a chloride-pumping bacteriorhodopsin mutant. *Biochemistry* **45**, 10633–10640 (2006).
27. Shibata, M., Yoshitsugu, M., Mizuide, N., Ihara, K. & Kandori, H. Halide binding by the D212N mutant of bacteriorhodopsin affects hydrogen bonding of water in the active site. *Biochemistry* **46**, 7525–7535 (2007).
28. Furutani, Y., Fujiwara, K., Kimura, T., Kikukawa, T., Demura, M. & Kandori, H. Dynamics of dangling bonds of water molecules in *pharaonis* halorhodopsin during chloride ion transportation. *J. Phys. Chem. Lett.* **3**, 2964–2969 (2012).
29. Maréchal, A. & Rich, P. R. Water molecule reorganization in cytochrome *c* oxidase revealed by FTIR spectroscopy. *Proc. Natl. Acad. Sci. USA* **108**, 8634–8638 (2011).